International Journal of Machine Learning and Image Processing (IJMLIP), Vol 1, Issue 1, April 2023.

Breast Tumor Classification Using Hybrid architectures (Googlenet, Alexnet, VGG16)

Sri Geetha M, Assistant Professor II, Department of Artificial Intelligence and Data Science, Kumaraguru College of Technology, Coimbatore- 641049 , mailsrigeetham@gmail.com

Abstract

Breast cancer is a kind of cancer that develops in the breast cells. Segmentation of breast tumor is a critical task. Segmenting tiny tumours in ultrasound images may be difficult owing to speckle noise, the fact that tumour forms and sizes might differ across individuals, and the presence of imaging areas that resemble tumours. In the area of biomedical image analysis, advanced learning-based algorithms have recently experienced a lot of success; nevertheless, one of most modern approaches that are now accessible have a poor track record whenever it relates to properly separating small breast cancers. This article presents a novel method to detect breast cancer at early stage. The proposed method combines the three architectures namely alexnet, googlenet and VGG. The total number of images utilized in this research came from two sources: small scale MIAS gave 576 images, and INbreast contributed 1095 images. According to the findings, the strategy that was presented gets the best overall performance and exceeds every other approach when it comes to the segmentation of tiny tumours. We aim to develop an approach to the problem of the (FDC) Feature Dimensionality Curve for the profound highlights that are obtained through the exchange learning pre-prepared CNNs. This structure is dependent on having previously created deep convolutional systems in addition to having a worldview that is based on univariate-based huge information. While removing shallow and profound aspects from INbreast mammograms, the deep - learning systems AlexNet, VGG, as well as GoogleNet are arbitrary choices that are employed. In terms of accuracy, loss rate, and runtime, GoogleNet outperformed AlexNet, PSO-MLP, and ACO-MLP, achieving 99% accuracy, the lowest loss rate (0.1557), and the shortest runtime (4.14 minutes).This performance seems to be advantageous for developing a computer-aided diagnostic (CAD) framework that is both practical and trustworthy for breast tumour categorization.

Keywords: deep transfer learning;breast ultrasound; feature reduction andselection;deep learning; feature dimensionality curse (FDC); tumor segmentation;CAD system;small tumor-aware network breast tumor

1. Introduction

According to projections made by the World Health Organization (WHO), [1] there will be around 2.3 million clinically detected occurrences in breast carcinoma in females across globe in year 2020. Because of the sickness, this led to the deaths of 685,000 people. It's also anticipated that by the time the year 2020 comes to a close, there will have been around 7.8 million surviving women who were identified as having breast cancer during the first five years of one's diagnosis. This figure was derived from previous research., which makes it the most prevalent type of malignancy found all over the world. As a result, it will become the more prevalent kind of malignancy in the whole globe. Such estimation is based on the observation that such proportion of women who get a diagnoses of breast carcinoma during the initial five decades after its first diagnosis increases by a factor of two every single year. The use of radiotherapy is an essential component of the cancer treatment process, which might additionally include ultrasound [3] and appealing reverberation imaging. Mammography with a higher level of sophistication is also an option. These approaches might potentially be included into the treatment of

breast cancer that has advanced. When breast cancer is detected in its earlier stages, radiation treatment has the potential to save a woman the need for a mastectomy. Because of breast density, radiologists could make an incorrect diagnosis of thirty percent of all breast malignancies [4]. Even seasoned radiologists have difficulty

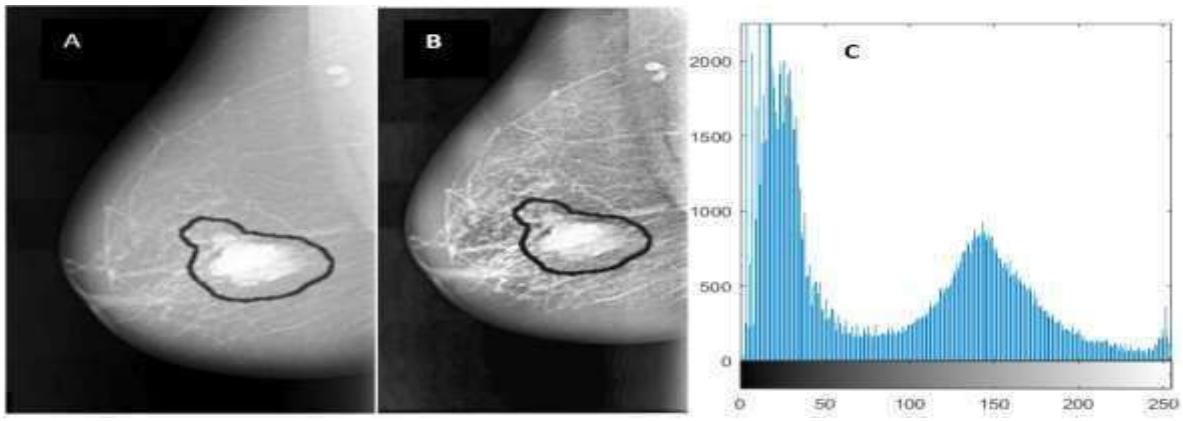

Figure 1 Breast Cancer Detection and the histogram of the same image

correctly interpreting a significant number of screening mammograms. One of the most important tools for identifying medical conditions using imaging is computer-aided diagnosis, or CAD. CAD stands for computer-aided diagnosis. It is a diagnostic tool that is based on artificial intelligence and was first created to assist radiologists in the process of evaluating medical pictures and indicating probable areas of concern [5,6]. The breast cancer affected image is shown in figure 1. It also displays the image intensities.

The artificial intelligence process known as convolutional brain organisations, or CNNs, requires the establishment of a great amount of boundaries in need to operate correctly. The number of tests that need to be prepared is often measured in the millions [7,8]. As a result of not enough clinical databases accessible, motion teaching is usually used to training CNNs to identify the profound features which are included in clinical imaging [9]. This is done because there are not enough clinical datasets available. Transfer learning entails making use of previously acquired information that is still relevant [10,11]. In 2016, a wide assortment of pre-prepared CNN learning models were made accessible, some of which are as per the following: VGG [15], GoogLeNet [13], AlexNet [12], ResNet [14], and Beginning V3 [16].

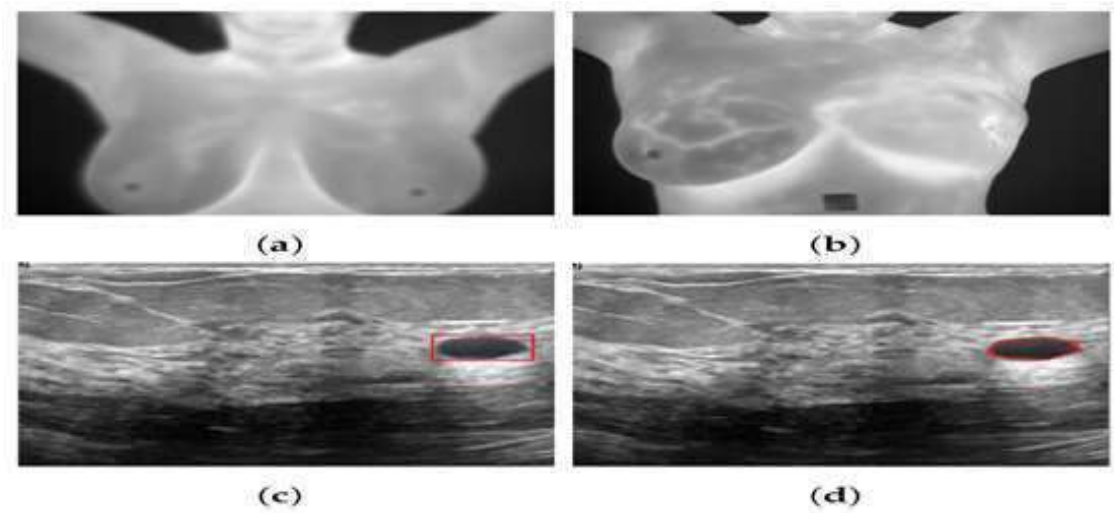

Figure 2 Applying Deep Learning on Breast cancer detection

Deep learning plays an important role to detect breast cancer and is shown in figure 2. Alternatively, as can be shown in Figure 3, they were not successful in attaining a decent performance when segmenting tiny tumours.

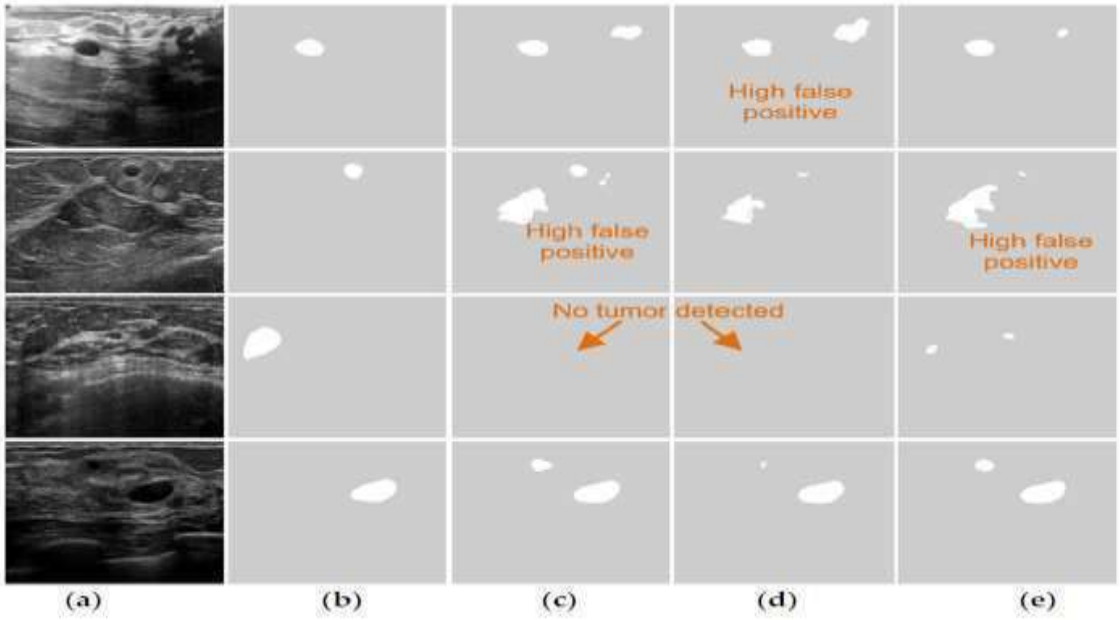

Figure 3 A method of dividing breast tumours into different-sized portions.GT: Ground truth. (a) BUS Image; (b) GT; (c) DenseU-Net; (d) CE-Net; as well as (e) RDAU-Net.The bolts emphasise Transport images where there is no discernible growth.

The remaining of the article is organized as follows: Section 2 discusses the related work. The methodology of the proposed system is described in section 3. Section 4 discusses the output results and the comparison graphs. The article is concluded in section 5.

2. Related Work

Breast carcinoma seems to be 2nd largest reason of mortality among females and affects 12.5% of females over the world. A new research concluded that timely detection of breast tumors is critical since it has the potential to cut the risk of death by up to 40 percent. An imaging test performed by a medical professional is the most accurate method for diagnosing breast cancer. However, magnetic resonance imagery (MRI), sonography, as well as digital mammogram are a few of the imaging technologies that are used for the confirmation of breast cancer. Imaging performed with digital mammography has the potential to be regarded as the foremost important method for earlier detection., but these are not the only imaging modalities that are used. About the categorization of breast cancer as well as its early detection, mammography has a number of problems that have been overcome by using machine learning. These problems include a restriction in identifying changes brought on by cancer as well as false positive rates and arbitrary assessments.

A large number of normal/tumor samples are necessary to create efficient prediction models. It may be challenging to gather the necessary preparatory material and build effective learning procedures whenever it refers to clinical applications like breast mammography, for example. As a consequence of this, it is strongly recommended to do the necessary preparations in the shortest amount of time and with the least amount of effort as is reasonably possible. In these circumstances, it would be beneficial to adapt the data received through one operation to the task that is anticipated to be done. Because of transfer learning, a model that was created in one location might sometimes serve as a point of convergence for learning in another. Mammography classification has made substantial use of transfer learning to enhance CNN designs. The main benefits of transfer learning include increases in categorization

accuracy, precision, and training speed. The categorization of mammograms has improved because to the fusion of retrieved deep characteristics.

The aspect space of the removed profound sections through the usage of move learning has the potential to be fairly extensive, since the number of deep highlights is dependent on the design and the number of layers of the pre-prepared CNN being employed. As far as our knowledge allows, very few investigations have made use of move learning in an effort to combat the Plague of Fractal dimension set on by the recovered deep highlights. Head part analysis (PCA) has been employed to aggregate the area of the recovered deep highlights before they have been presented to a conventional classifier known as the Help Vectors Machines (SVM). The use of principal component analysis (PCA) to decrease the component area for motion learning-recovered highlights was initially recommended in. Since that time, it has demonstrated outcomes with greater grouping precision than those achieved by utilising fundamentally eliminated profound parts.

Samee et al. in gave one more commitment to handling the issue of the Scourge of Dimensionality of the recovered profound elements by helping the presentation of PCA through the utilisation of Strategic Relapse to decide the significant guideline parts acquired from the PCA examination. This was done to determine the significant guideline parts got from the PCA examination. Our inventive approach towards picking the greatest remarkable important deep highlighting from the ones recoverable mostly by or before CNNs while it is given on breast mammogram of whether safe or dangerous malignant tissue was motivated by the criteria that have recently been shown.

3. Methodology

Convolutional Neural Network (ConvNet)

Biologically inspired, CNN is a special kind of feed forward network. by their sparse connection and weight sharing between their neurons. Unlike other DL algorithms, it allows input data in two dimensions. The whole organisation will get a picture contribution with the dimensions (h,w,c), while H represents for level, W stands for body mass, and C represents for the amount of directives included in the image. This device is referred to as a CNN. Such networks basically provide the limited likelihood allocation throughout the subcategories p(y|x) & are known to as the clear (RGB) shades. A succession of the nonlinear level image is used to accomplish this. The kernel multiplies each pixel in an image by the opposite kernel pixels, along with any neighbouring pixels that it covers. After a totaling of the items, the result is used to determine the value of the convolved picture pixel that corresponds to the original image's beginning pixel.

There are three levels in the CNN architecture. Three standard pooling levels in succession, the last of which is completely linked.

The primary layer of a ConvNet and the one with the highest computing demand is the convolutional layer. Its primary job is to take the pixels of the input picture and extract its characteristics. ConvNet's first layers may extract features at lower levels. The characteristics that can be retrieved from the convolutional layers continually grow as the network develops to a deeper degree. The input and filter are multiplied element-by-element in the computation, which is then added up. The alleged Channel, which is also known as the Part, may be viewed of as a glass that is cushioned on the image and is made up of several loads. In order to create a convolution, the value of every pixels in the browser's covering region is copied and then increased by the mass of the glass at its correlating position. This is why the layer is called a convolution layers.

We present a flowing highlight determination strategy for picking non-repetitive and critical aspects. This review is a continuation of the research that we did before on the classification of breast malignant growths by the use of motion learning. The use of two different flowing FS stages allows for the component selection process to be carried out successfully. In breast mammograms, the first stage is to use convolutional neural networks (CNNs) like GoogleNet, VGG, as well asAlexNet to distinguish between shallow and deep components in the area of concern. This is done to ensure that the final findings are reliable.

Figure 4. Determination for grouping bosom illness is included in the structure for deep learning-based flows.

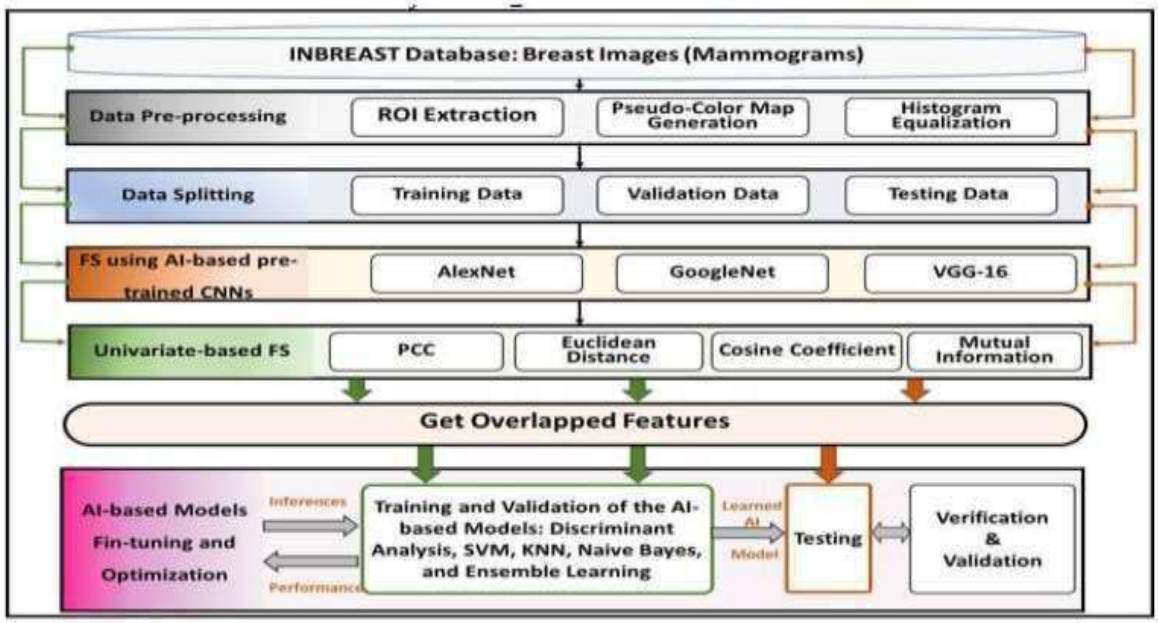

3.1. ROI Extraction and Images Pre-Processing

This analysis made use of information obtained from a number of public sources, including the INbreast, which is well-known for its provision of information on full-field, high-goal advanced mammography. In addition to the sources that have previously been cited, information was gathered from a wide range of public sources for the purpose of this inquiry. In order for a mammogram to be considered for inclusion in the INbreast data collection, it must have been acquired at a Breast Community that was housed inside a College Emergency clinic. Only then would the mammography be eligible for consideration. The INbreast data collection incorporates a total of 410 mammograms into its database for analysis. Mammograms like this have been linked to the medical records of 115 different individuals. The INbreast dataset contains the appropriate analysis for each and every mammogram, as well as the areas of each image that are most likely to include irregularities. In addition, the dataset identifies the regions of each picture that are most likely to contain abnormalities. For each injury, the centre and breadth of the surrounding circle are used to illustrate these places. In a similar manner, the proper judgement has been made for each and every mammogram that is included in the dataset. In order for us to carry out our tests, we first chose out areas of interest (ROIs) of 32 by 32 squares within the lesion. Keeping the region of interest (ROI) as small as feasible while simultaneously delivering a sample that was statistically typical of the lesion made it easier for the devised strategy to achieve superior localization performance. The aberrant areas were selected by hand from among the lesions that were accessible in order to exclude any risk of bias. The examples reflected the different anomaly subclasses and had sore or bunch measurements that were enough to include the optimum return on initial capital investment size in their inclusion. In addition, the examples were included. In addition to this, the instances demonstrated a wide range of initial capital investment quantities. We have only just

established what is known as a strategy that is beneficial for the pre-handling of these datasets, and that approach is called pseudo-variety planning. The accuracy with which lesions on mammograms are grouped together is significantly impacted by the use of this approach. This was made feasible by the fact that the approach featured the ability to boost the chance of recognising injuries that were similar to one another. This made it possible to identify injuries that were similar to one another. "Pseudo-variety" programming might transition between all three of the available information channels in order to deliver the most up-to-date information possible while the viewer is watching CNN. This would ensure that the viewer is receiving the most current information possible (Red, Green, and Blue).

3.2. Feature Selection Using Pre-Trained CNNs and the Univariate-Based Approach

Layers that are convolutional, pooling, and totally related may be found in CNNs that have already been created (FC). When the convolution layers have finished their work, the totally associated layer will come in and group the recovered attributes. In this research, both benign and malignant breast cancer images were processed via the convolutional and pooling layers of convolutional neural networks (CNNs).This was done in order to facilitate comparison between the two types of images. CNN's pre-prepared image classifiers, such as AlexNet, VGG, and Googlenet, have gained a lot of notoriety in recent years. Alex Krizhevsky and his colleagues made an excellent presentation about AlexNet at the ImageNet Enormous Scope Visual Acknowledgment Contest in 2012. (ILSVRC). Their previous versions of CNN have been upgraded with additional layers. They have mistake rates that are in the top five in the ILSVRC competition. As can be seen in Figure 5, AlexNet is comprised of the following layers: an input picture layer with dimensions of 227 by 227 by 3, The architecture of the neural network is comprised of the following layers: a result layer that is a SoftMax layer, 5 convolution levels, three maximal pooled layers, two completely associated (FC) layers, and five fully associated (FC) result layers. The first convolution layers is made up of 96 channels or sections which are evenly dispersed throughout an area that is 11 pixels wide and 11 pixels tall. This region has a height of 11 pixels and a width of 11 pixels. When the output of this layer has been normalised via the response normalisation, an overlapping max pooling layer will take its place. The second convolutional layer has 256 kernels that are each 5 x 5, and the output is then normalised and pooled using the identical methods that were described in the first paragraph. The third, fourth, and fifth convolutional layers each have a design that is generally similar to one another, and they each have 384 channels with sizes that are three by three. Moreover, the third, fourth, and fifth convolutional layers all have the same number of layers.

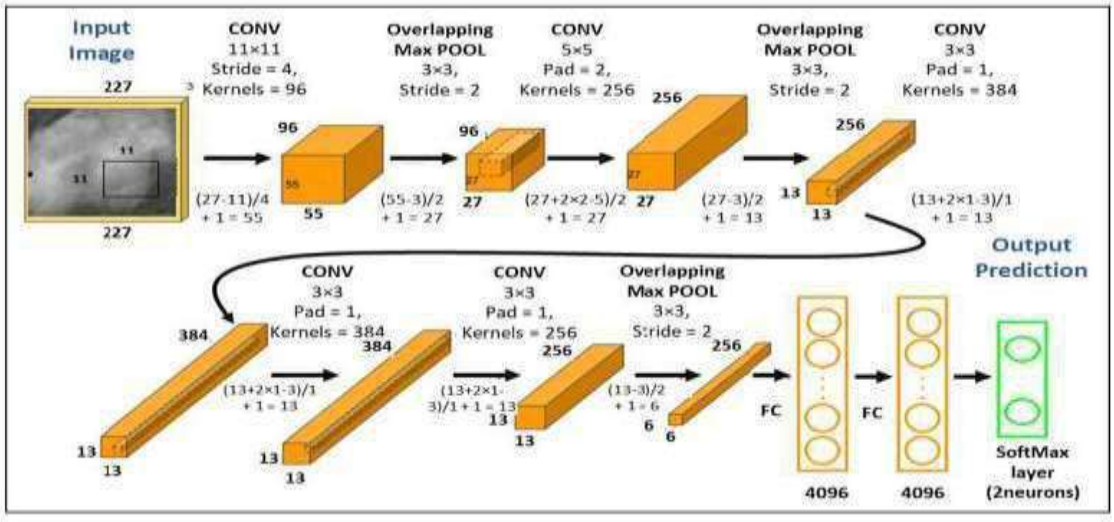

Figure 5. AlexNet flowchart architecture.

In 2014, Andrew Zisserman and Karen Simonyan were the ones who first presented the VGG. While using VGG, the accuracy of the CNN is impacted by the size of the network. The ReLU activation step occurs after the convolutional layers but before the pooling step. As can be seen in Fig. 6, the VGG 16 architecture is quite simple. It has an input layer that can capture pictures that are 224 pixels by 224 pixels by three pixels. After the input layer comes a series of layers of convolution processing that have been layered one on front of the other. Each convolutional layer consists of a series of three-by-three-pixel filters of modest sizes. It is feasible to add an unlimited number of convolutional layers to the VGG architecture because the convolutional sections have such a tiny size. This has helped to enhance the entire appearance of these businesses, which is a result of the improvement. Then come three layers that are completely linked, which come after the stack of convolutional layer. The initial two F-C layers all have a total of 4096 neurons, however the third FC layer only contains two neurons. These two neurons are accountable for the paired arrangement of the mammogram's various kinds of tissue due to their role in the process (ordinary, and unusual). When all of the other steps have been completed, a delicate max layer that has aspect ratios of 1 by 1 by 2 is applied. As can be seen in Figure 7a, an inception module consists of a maximum pool layers of size

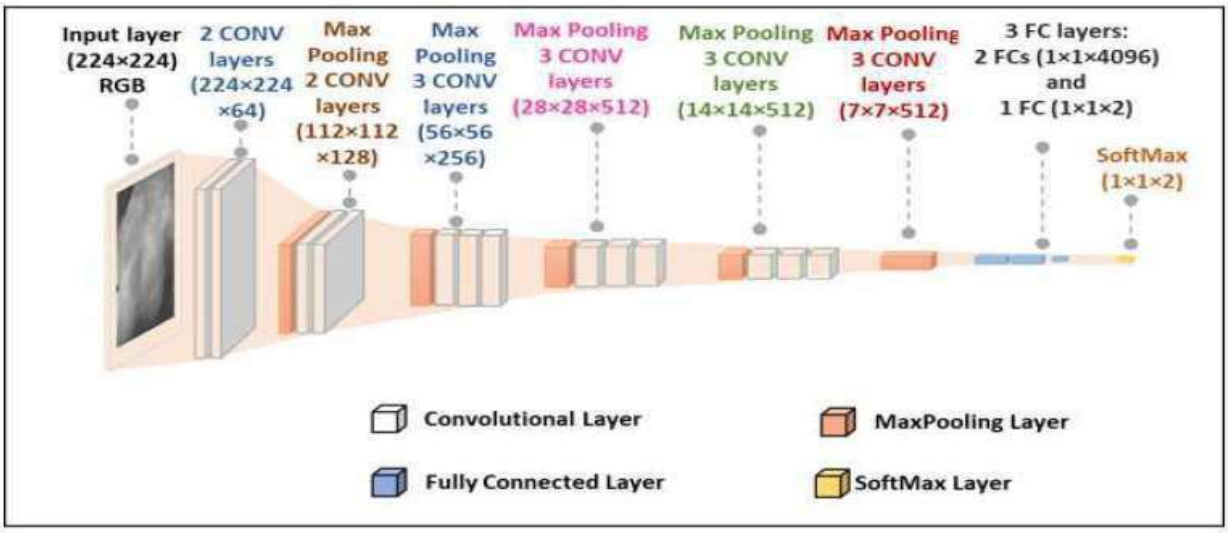

Fig. 6.flowchart architecture of Pretrained CNN, VGG16.

3X 3 as well as three convolutional layers of sizes 1 x 1, 3 x 3, and 5 x 5, all of which operate in parallel with one another. The convolutional layers are denoted by the colour grey.

Once the input from previous layer is received by the inception module, which then performs its parallel processes, the output feature maps are then concatenated, and the information is given on to module that comes after it. Using this strategy results in a more extensive network. The processing of the inception module has been simplified thanks to the implementation of a 1 x 1 convolution, which is shown in Figure 5b and applied to the module's internal layers. In the deep network that is NIN, the 1 1 convolution has been implemented. Global average pooling is carried out just before the FC layer. The input layer, convolutional layers, max pooling, inception modules, FC, and softmax layers are some of the components that are included in the overall architecture of GoogleNet, which has a total of 22 layers. The fact why GoogleNet is simpler to train than AlexNet is due to the fact that it has 12 less parameters.

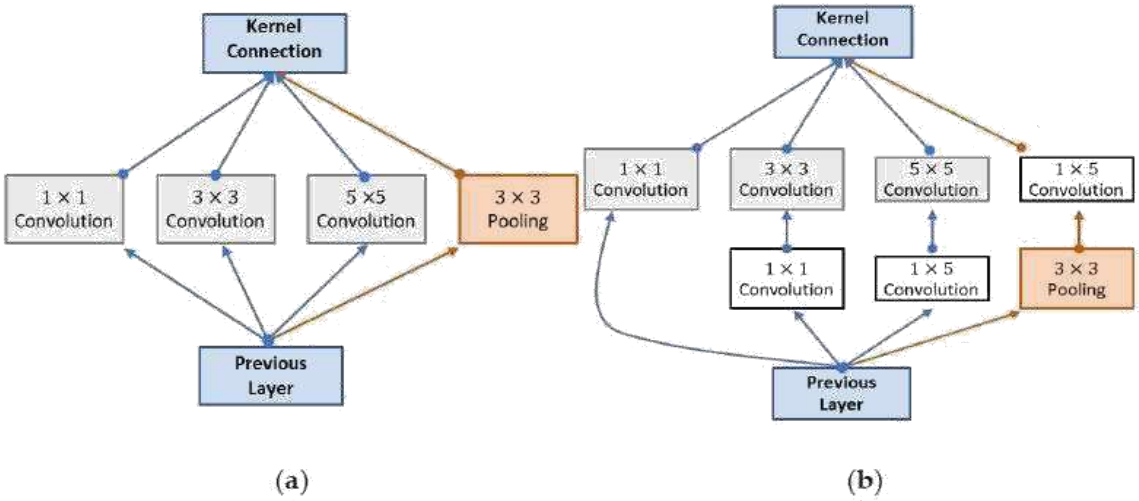

Fig. 7. A starting point for the GoogleNet DCNN's origin module. (a) A root module that does not contain a 1 by 1 convolutional layer. (b) Origin modules that has a convolutional layer with dimensions of 1 by 1.

The stochastic angle plunge with energy (SGDM) streamlining agent will be used in this assessment with the learning restrictions that are presented in Table 1. After the observation of the results of the approval via testing, these limits were found, these were used by all companies, allowing for a side-by-side comparison of results and computing costs.

Table 1. The values of the learning parameters that are used while training previously trained CNNs.

Learning Parameters	Value
Learning rate	0.0001
Number of training epochs	400
Batch size	16
Momentum factor	0.9
L2-Regularization	0.0005

While picking a feature subset (FS), it is vital to remove any features from the system that are either redundant or do not serve a purpose. The feature subset that is ultimately selected should, in line with the standards of some objective function, be the one that results in the greatest degree of performance. FS is what's known as NPhard issue, that simply mean that finding a solution to it in a non-deterministic polynomials period of time is very challenging. Highlight choice has developed into a fundamental component that should be available prior to the development of competent ML models as a result of the growing volume of data that has needed to be handled over the course of the past couple of years. This is because the volume of data that has needed to be handled has been growing steadily.

The methods of element determination, as opposed to the methods of include extraction, do not have any impact on the fundamental representation of the data. Both the process of extracting elements and the process of determining their properties have the goal of avoiding overfitting the data to the extent that is possible given the circumstances. This is done in order to ensure that subsequent learning is as efficient and precise as possible. Filtering, wrapping, and embedding are the three categories into which FS methods might be placed. The FS approach that uses filters to obtain features from data does not need any learning on the user's part. Wrappers utilise machine learning (ML) techniques to figure out which characteristics are helpful.

The findings provided evidence that is indisputable and cannot be contested. This served as the impetus for investigating practicability of unqualified combination models univariate channel based FS selecting the primary highlights from the separated arrangement of elements produced by pre-prepared CNNs in order to categorize breast sores as either safe or dangerous. This allowed us to classify breast sores as either harmless or dangerous. The technique of determining an on/off ideal component, the benefits of which vary between normal and obsessive situations, is the major focus of attention here. Figure 8 should make it clearly clear that the investigation that is now taking place makes use of two good traits, as this should be the case because it is being used.

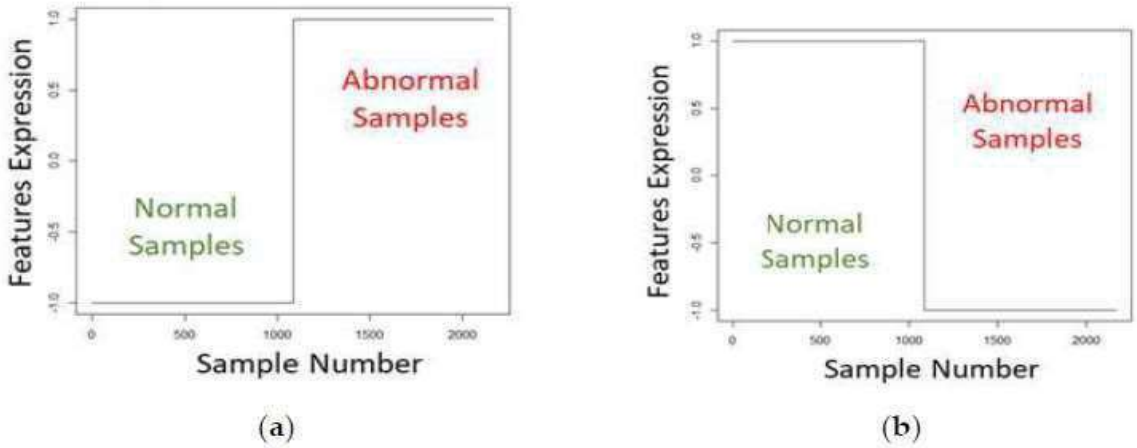

Fig. 8. The on or off position of ideal feature. (a) Ideal features (upregulated). (b) Ideal features (downregulated).

From that point forward, the component separation method will progress to the second phase, during which the extricated include grid (EFM), which was produced by the pre-prepared CNNs, will be used. The strategy of using z-scores was used in order to effectively finish the work of normalizing the EFM's multiple components in its entirety. The standardized characteristics all have a standard deviation of one and are not focused on any one specific characteristic or value. The number one is used to denote the standard deviation of the characteristics that have been standardized. The Z-score of an irregular component is calculated by using condition, which takes into consideration both the element's mean value M and its standard deviation. An irregular component is denoted by the letter F in (1).

$$Z_{score} = \frac{\mathrm{F} - \mathrm{M}}{\sigma} \quad (1)$$

The correlation coefficient of Pearson, that is apparent in the Conditions table, reveals that there is a significant (2), is a metric that may be used in order to ascertain the degree of resemblance that exists between an ideal feature mentioned by FIdealas well as particular feature mentioned by F.

According to it, compare two different groups of values.

$$r = \frac{\sum_{i=1}^{S}(F_i - \overline{F})\,(F_{Ideal_i} - \overline{F_{Ideal}})}{\sqrt{\sum_{i=1}^{S}(F_i - \overline{F})^2}\,\sqrt{\sum_{i=1}^{S}(F_{Ideal_i} - \overline{F_{Ideal}})^2}} \quad (2)$$

Estimating the space-based distance that separates two vectors from one another may be used as a method for doing a proximity assessment between the vectors. As a consequence of this, we decided to apply the Euclidean distance in our investigation of the optimum component, also known as FIdeal, to each of the several highlights in the EFM. The magnitude of the component lattice that was extracted may be inferred from the value of the variable S. The graphics Fi and F, taken independently, represent, respectively, the value of a component in each specific example that is provided (I), as well as the component's mean value over all the input tests. FIdeal I addresses the value of the ideal component

test I, while FIdeal addresses the mean value of this component over all input tests. Nevertheless, FIdeal I addresses the value of the ideal component test I. FIdeal further discusses the significance of the value of this component. The cosine coefficient is one tool that may be utilized in the EFM to evaluate the degree of dependence that exists between the best element as well as a given feature called Fi. This is shown by the equation shown below (3). By examining the cosine coefficient, one is able to determine whether or not 2 angle is heading in the similarpath. If the cos coefficient shows 0, this indicates that the angles are independent of one another.

$$r_{\text{cosine}} = \frac{\sum_{i=1}^{S}(F_i - \overline{F})\, F_{Ideal_i}}{\sqrt{\sum_{i=1}^{S}(F_i - \overline{F})^2}\sqrt{\sum_{i=1}^{Q} F_{Ideal_i}^2}} \quad (3)$$

It is also possible to choose the important features by making use of the information that is shared between the most important component, FIdeal, and the other highlights included in the EFM. Condition (4) provides the formula for registering common data. In this condition, the H(FIdeal) variable addresses the entropy of the best component, and the H(FIdeal| F) variable addresses the contingent entropy among FIdeal and an element, F, in the EFM. Both of these values are in the EFM.

$$I(F_{Ideal}, F) = H(F_{Ideal}) - H(F_{Ideal}|F) \quad (4)$$

3.3. Classification and Model Assessment

In order to provide an appropriate solution to this request, a quantified artificial intelligence framework was used, and as part of that framework, the development of six significant sorts of typical classifiers was carried out. These classifiers were utilized in order to organize the information that was gathered into the appropriate categories. When I think of this group of approaches, some of the ones that springs decision trees, credulous Bayes, SVM, discriminant analysis, KNN, and gatherings. Further examples of these methods are gatherings. Each and every one of the countless borders and variations that are comprised by each classifier was modified in order to get the best possible presentation while also reducing the issue of overfitting to the greatest extent that was practically possible.

4. Results and Discussion

We provide a basic architecture of a PC-supported diagnostic system for the collection of breast disease bruising in this research. The system makes use of streaming periods of pre-arranged CNNs and certified mix model univariate-based FS approaches. In order to investigate breast illness, this framework was developed. This architecture is dependent on univariate approaches and makes use of CNNs that were established at an earlier stage than they are now used. The process is broken up into four parts: first is the data organization, then comes the feature assurance with the utilization of CNNs, and last comes the collection. In, we presented an early portion of the concept of applying pseudo-concealed wishing to work with the accommodation of information images to pre-arranged CNNs. The comparison of breast cancer detection in early stage is shown in figure 9.

On INbreast, pseudo-tinted arranging was carried out, and the sensitivity of the recently developed PC-supported plan system is being evaluated in relation to the pseudo-concealed photos that were produced by the preparation. At the point in the FS cycle that is considered to be the middle, the sending of pre-arranged CNNs has taken place. The areas of premium (returns on capital contributed) The associations in each dataset were enlarged using bilinear expansion with an adversarial channel to adapt to their respective sizes (224 224 for the VGG/GoogleNet and 227 227 for the AlexNet).The purpose of this was to achieve the ultimate goal of meeting conclusions, protecting picture quality, and keeping them free of partner relics. This was accomplished taking into consideration the fact that the data layer is an essential part of the content covered in the trade educational experience and cannot be altered in any manner. It is required to establish the learning parameters before beginning training on a CNN that has already been trained. In this particular investigation, It was determined to make use of a

stochastic slope drop with energy enhancer (SGDM). The L2-regularization setting was dropped to 0.0005, the force term factor was set to 0.9, and the learning speed was lowered to 0.0001 on this enhancer and the slope limit method

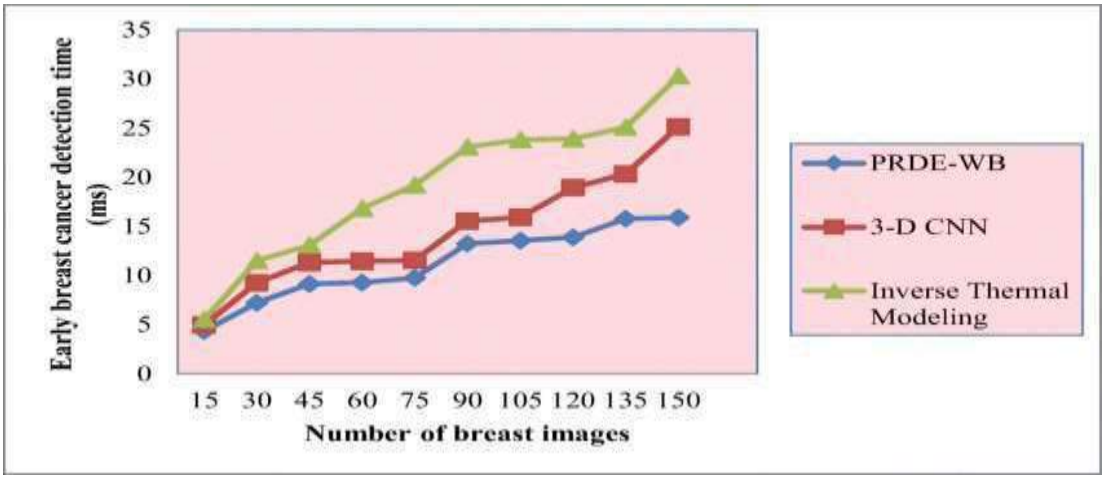

Figure 9 Comparison of early breast cancer detection

was modified to use the L2-standard technique. The biggest number of participants who could participate in the event at one time was 16, while the maximum number of people who could participate in the event at any one time was 400. The results of the validation tests conducted with running were used to guide the decision to go with these alternative training methods. These were applied to each and every network to make it possible to do a direct comparison of the outcomes obtained by each network. The amount of characteristics that can be retrieved from a network is said to be affected by the topology of the network, as was reported in. Using AlexNet, GoogleNet, and VGG16 one at a time helped extract a total of 4096, 1024, and 4096 items from the data, respectively.

Both the ML tool store and an academic version of MATLAB 2020a were used throughout the events. Also, the test that was carried out was successful. The Intel® CoreTM i7-6700HQ is the primary processor that is used in the PC architecture. This processor is created by Intel, has a total of four processing cores, operates at a frequency of 2.60 gigahertz, and runs at 2.60 gigahertz. In addition to this, the device is equipped with a graphics processing unit (GPU) that is compatible with CUDA and has a maximum memory capacity of 16 gigabytes (Smash) (NVIDIA GeForce GTX 950M with 4 gigabytes of memory). In any event, Notwithstanding the fact that the investigation's results will vary depending on the specific hardware and setting to which it is being applied, to, the general characteristics that were gathered from the tests can still be used to evaluate and differentiate between the various philosophies. This is the case despite the fact that the findings of the investigation are subject to the machine and environment that is being alluded to. This is the case despite the fact that the results of the inquiry are dependent on the machine and the environment that is being referred to in the sentence.

Classification Model Construction and Evaluation

In last stage in the proposed CAD architecture, the top twenty most relevant characteristics is then sent to 6 unique family for classifier classicals to be analysed. These traditional groups of classifiers include of decision trees, discriminant analysis, support vector machines, key-value networks, naive Bayes, and ensembles. We carried out a total of five separate tests in order to investigate and evaluate the effectiveness of the recently developed computer-aided design framework. In particular, we were interested in assessing how successfully it performed the duties that were assigned to it and whether or not it lived up to our expectations. The elements that have been recovered from pre-prepared CNNs (AlexNet, VGG, and GoogleNet) are placed through one strategy for the univariate channel-based FS approaches before being offered to the old-

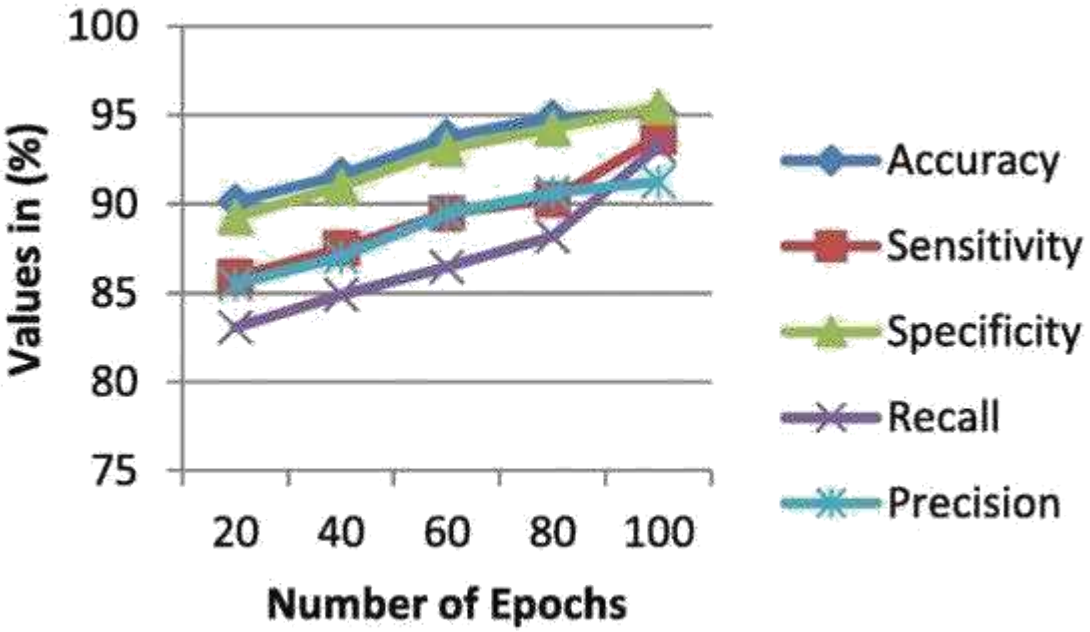

Figure 10 Performance metrics of the proposed system

style classifiers. This occurs before the elements are provided to the classifiers (PCC, CC, ED, and MI). This is done in each test to measure the amount of similarity between the components that have been recovered from pre-prepared CNNs and the ideal highlights. This helps determine how close the highlights get to the original. This takes place before the objects in question are presented to the classifiers who adhere to the time-honored method. This is done before the components are brought in so that an order for them can be placed using the traditional methods. This process is now complete, and now we can check to see whether the highlights that have been This is done before the components are brought in so that an order for them can be placed. The performance metrics of the proposed system is shown in figure 10.

At the final phase of the test, a crossover selection of the recoverable characteristics from each of the univariate FS approaches is used for the categorization of the breast tissues. This ensures that the most accurate results are obtained. Table 2 displays the outcomes of the studies that were carried out on the INbreast dataset, along with the possible ramifications that may be derived from those outcomes based on the findings shown in the table. Just the findings that were acquired from the models that had the highest overall performance are included in Table 2.

Table 2. Appraisal of old-style classifiers prepared on all univariate-put together component determination techniques with respect to the removed element grid (EFM) from the CNN. The gathering (sub-space KNN) classifier assesses this.

Pre-Trained CNN for Feature Extraction	Univariate Feature Selection	TP	TN	FP	FN	Accuracy (%)	Sensitivity(%)	Specificity (%)	Precision (%)	False Negative Rate (%)	False Positive Rate (%)	AUC	Matthew's Correlation Coefficient	F1-Score (β = 1)
AlexNet	PCC	1051	1074	10	33	98.00	96.96	99.08	99.06	3.04	0.92	1	0.9605	0.9800
VGG16		1050	1066	18	34	97.60	96.86	98.34	98.31	3.14	1.66	1	0.9521	0.9758
GoogleNet		1007	1042	42	67	95.00	93.82	96.13	96.03	6.18	3.87	0.98	0.8907	0.9491
AlexNet	CC	1050	1072	12	34	97.90	96.86	98.89	98.87	3.14	1.11	0.99	0.9578	0.9786
VGG16		1035	1063	21	49	96.80	95.48	98.06	98.01	4.52	1.94	1	0.9337	0.9673
GoogleNet		1018	1037	47	66	94.80	93.91	95.66	95.59	6.09	4.34	0.99	0.8959	0.9474
AlexNet	ED	765	1084	80	321	81.50	70.39	92.62	90.53	29.61	7.38	0.95	0.6482	0.7919
VGG16		760	1089	75	324	81.60	70.11	93.06	91.02	29.89	6.92	0.94	0.6493	0.7921
GoogleNet		957	1018	66	127	91.10	88.28	93.91	93.55	11.72	6.09	0.98	0.8233	0.9084
AlexNet	MI	1054	1065	19	30	97.70	97.23	98.25	98.23	2.77	1.75	1	0.9548	0.9773
VGG16		1018	1057	27	66	95.70	93.91	97.51	97.42	6.09	2.49	0.99	0.9148	0.9563
GoogleNet		999	1040	44	85	94.00	92.16	95.94	95.78	7.84	4.06	0.98	0.8816	0.9394
AlexNet	Hybrid	1063	1073	11	21	98.50	98.06	98.99	98.98	1.94	1.01	1	0.9705	0.9852
VGG16		1043	1059	25	41	97.00	96.22	97.69	97.66	3.78	2.31	0.99	0.9392	0.9693
GoogleNet		1006	1044	40	78	94.60	92.80	96.31	96.18	7.20	3.69	0.99	0.8917	0.9486

According to the findings, 24 of the cases that were benign or normal were properly categorised, 32 of the instances that posed a danger were correctly evaluated, whereas seven of the cases that posed a threat were incorrectly classified as innocuous or typical. Although six of the cases were incorrectly labeled as harmful, 32 of the cases that posed a threat were correctly examined (Table 3).

Table 3. AlexNet classification results.

Prediction Category	Genuine Category	
	B or N	M
B or N	24	7
M	6	32

In Table 4, we can see the differences between the results obtained with the handmade surface, morphological, and joined surface and morphological elements, the results obtained with the calibrated VGG19 model, and the results obtained with and without the highlights choice for the CONV include set.

The outcomes of the predictions made with dataset 2 using a number of different deep learning networks are shown in table 5. The time required for training MobileNet-v2 was 28 minutes and 38 seconds, and it achieved the greatest accuracy (96.84%). DenseNet201 spent the greatest time preparing (132 minutes and 25 seconds) and had the highest accuracy (96.01%), whereas AlexNet spent the least time preparing (3 minutes and 4 seconds) and had the lowest accuracy (79.89%). Starting ResNet-v2 had the lowest accuracy (79.34%) and required the longest amount of time spent in advance preparing (106 minutes and 48 seconds). The modified AlexNet with move learning achieved higher grouping accuracy than previous deep learning systems. making it acceptable for the categorization of HMI images**.**

GoogLeNet	81.02%	7 min 48 s	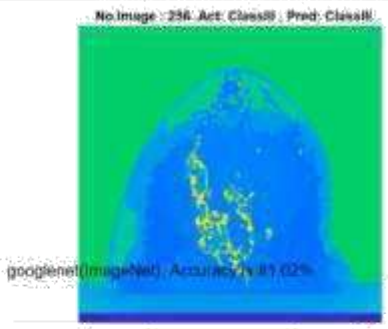
AlexNet	80.33%	5 min 39 s	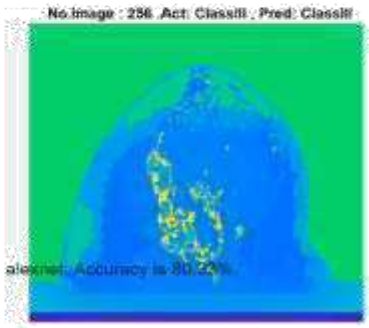

Figure 11 Accuracy comparison of Alexnet and Googlenet

5. Conclusions

According to the data that were reported in this study, the CONV highlight set may offer the greatest potential grouping performance that can be achieved by using deep highlights. The capabilities that are shown here comprise highlights that have been taken from all of the convolutional layers that are a part of the VGG19 model. The findings of the analysis substantiated this assertion. When the CONV highlight set and morphological characteristics were merged, the normal MCC was 92.0 percent, the typical PPV was 95.1 percent, the typical NPV was 968.2 percent, and the typical exactness was 96.1 percent. These findings are comparable to the hand-tailored surface and morphological highlights, as well as the tweaked VGG19 model. The findings were discussed in the assessment that is still taking place at this time. Review findings examining the performance of the hypothesis suggest that the CONV highlight set, or a combination of the CONV highlight set and morphological features. The CAD system that was constructed using ROI classification exhibited promising results when compared to earlier work that used regular machine learning methods as well as deep learning-based approaches. Recovered exactness and awareness are equivalent to attributes that we had only recently arrived to performance of the hypothesis suggest that the CONV highlight set, or a combination of the CONV highlight set and morphological features. The CAD system that was constructed using ROI classification exhibited promising results when compared to earlier work that used regular machine learning methods as well as deep learning-based approaches. Recovered exactness and awareness are equivalent to attributes that we had only recently arrived to in our earlier work on the INbreast dataset. Research was conducted with the use of the INbreast dataset. we proposed a new highlight determination framework for choosing unique features to include in a computerized mammography-based categorization system for breast injuries. This was done so that we could more precisely categorize breast damage.

Reference

1. Breast Cancer. Available online: https://www.who.int/news-room/fact-sheets/detail/breast-cancer (accessed on 15 August 2021).

2. Sung, H.; Ferlay, J.; Siegel, R.L.; Laversanne, M.; Soerjomataram, I.; Jemal, A.; Bray, F. Global Cancer Statistics 2020: GLOBOCANEstimates of Incidence and Mortality Worldwide for 36 Cancers in 185 Countries. CA Cancer J. Clin. 2021, 71, 209–249. [CrossRef][PubMed]

3. Mao, Y.-J.; Lim, H.-J.; Ni, M.; Yan, W.-H.; Wong, D.W.-C.; Cheung, J.C.-W. Breast Tumor Classification Using UltrasoundElastography with Machine Learning: A Systematic Scoping Review. Cancers 2022, 14, 367. [CrossRef] [PubMed]

4. Kolb, T.M.; Lichy, J.; Newhouse, J.H. Comparison of the Performance of Screening Mammography, Physical Examination, andBreast US and Evaluation of Factors that Influence Them: An Analysis of 27,825 Patient Evaluations. Radiology 2002, 225, 165–175.[CrossRef] [PubMed]

5. Cheng, H.; Shi, X.; Min, R.; Hu, L.; Cai, X.; Du, H. Approaches for automated detection and classification of masses inmammograms. Pattern Recognit. 2006, 39, 646–668. [CrossRef]

6. Atteia, G.; Alhussan, A.A.; Samee, N.A. BO-ALLCNN: Bayesian-Based Optimized CNN for Acute Lymphoblastic LeukemiaDetection in Microscopic Blood Smear Images. Sensors 2022, 22, 5520. [CrossRef]

7. Ayatollahi, A.; Afrakhteh, S.; Soltani, F.; Saleh, E. Sleep apnea detection from ECG signal using deep CNN-based structures. Evol.Syst. 2022, 322, 1–16. [CrossRef]

8. Custode, L.L.; Mento, F.; Afrakhteh, S.; Tursi, F.; Smargiassi, A.; Inchingolo, R.; Perrone, T.; Demi, L.; Iacca, G. Neuro-symbolicinterpretable AI for automatic COVID-19 patient-stratification based on standardised lung ultrasound data. J. Acoust. Soc. Am.2022, 151, A112–A113. [CrossRef]

9. Samala, R.K.; Chan, H.; Hadjiiski, L.; Helvie, M.A. Risks of feature leakage and sample size dependencies in deep featureextraction for breast mass classification. Med. Phys. 2021, 48, 2827–2837. [CrossRef]

10. Taylor, M.E.; Kuhlmann, G.; Stone, P. Transfer Learning and Intelligence: An Argument and Approach. Front. Artif. Intell. Appl.2008, 171, 326.

11. Parisi, G.I.; Kemker, R.; Part, J.L.; Kanan, C.; Wermter, S. Continual lifelong learning with neural networks: A review. Neural Netw.2019, 113, 54–71. [CrossRef]

12. Krizhevsky, A.; Sutskever, I.; Hinton, G.E. ImageNet Classification with Deep Convolutional Neural Networks. Commun. ACM2012, 25, 84–90. [CrossRef]

13. Szegedy, C.; Liu,W.; Jia, Y.; Sermanet, P.; Reed, S.; Anguelov, D.; Erhan, D.; Vanhoucke, V.; Rabinovich, A. Going Deeper withConvolutions. In Proceedings of the IEEE Computer Society Conference on Computer Vision and Pattern Recognition, Boston,MA, USA, 7–12 June 2015.

14. He, K.; Zhang, X.; Ren, S.; Sun, J. Deep Residual Learning for Image Recognition. IEEE Comput. Soc. 2016, 2016, 770–778.

15. Simonyan, K.; Zisserman, A. Very Deep Convolutional Networks for Large-Scale Image Recognition. In Proceedings of the3rd International Conference on Learning Representations, ICLR 2015—Conference Track Proceedings, San Diego, CA, USA,7–9 May 2015.

16. Szegedy, C.; Vanhoucke, V.; Ioffe, S.; Shlens, J.; Wojna, Z. Rethinking the Inception Architecture for Computer Vision. InProceedings of the IEEE Computer Society Conference on Computer Vision and Pattern Recognition, Las Vegas, NV, USA, 9December 2016; pp. 2818–2826.